Glucocorticoid effects on mouse microvascular endothelial barrier permeability are brain specific

Carola Förster[1], Jens Waschke[1], Malgorzata Burek[1], Jörg Leers[2] and Detlev Drenckhahn[1]

[1]*Institute of Anatomy and Cell Biology, University of Würzburg, Koellikerstrasse 6, D-97070 Würzburg, Germany*
[2]*Institute for Genetics, Justus-Liebig-University Giessen, Heinrich-Buff-Ring 58-62, D-35392 Giessen, Germany*

Endothelial cells (ECs) from different vascular beds display certain common qualities, but each subtype is uniquely adapted to meet the demands of the underlying tissues. The structural peculiarities of intercellular junctions are, for instance, considered to account for the differences in permeability displayed by various vascular beds: strong occludin expression is unique to cerebral ECs and considered to account for the high electrical resistance and low paracellular permeability of brain microvessels which constitute the blood–brain barrier (BBB). The integrity of the BBB is compromised in many disorders of the human CNS; therapeutic strategies include treatment with glucocorticoids (GCs), which improve barrier properties of the BBB. In contrast, positive effects of GCs on peripheral vascular permeability could not be demonstrated clearly, while side-effects of prolonged GC treatment are considerable. In an effort to elucidate this difference, we analysed the expression of occludin and the glucocorticoid receptor (GR) in BBB and non-BBB (myocardium) endothelial cells. Our results demonstrate complete GR downregulation by GCs in murine non-BBB endothelial cells *in vivo*, whereas GC administration led to nuclear concentration of GRs in BBB endothelium. In correlation with these *in vivo* data, the use of cerebral and myocardial endothelial cell lines proved GR downregulation in non-BBB cells *in vitro* in response to GC treatment. Divergent transactivating activity of GRs in the BBB and non-BBB endothelial cellular context could be demonstrated after transfection of endothelial cells with a model GC-responsive test promoter plasmid in the presence and absence of dexamethasone. Our results thus suggest differential signalling mechanisms involved in endothelial barrier regulation, arguing for the development of tissue-specific drugs for therapeutic applications.

(Resubmitted 30 January 2005; accepted after revision 15 March 2006; first published online 16 March 2006)
Corresponding author C. Förster: Institute of Anatomy and Cell Biology, University of Würzburg, Koellikerstrasse 6, D-97070 Würzburg, Germany. Email: carola.foerster@mail.uni-wuerzburg.de

Endothelial cells (ECs) from different vascular beds display certain common qualities, but each subtype is uniquely adapted to meet the demands of the underlying tissue. Endothelial cells show definite morphological and physiological variations that divide them into subtypes, each specifically associated to various categories of organs (Ghitescu & Robert, 2002). In particular, the structural peculiarities of intercellular junctions are considered to account for the differences in permeability displayed by various vascular beds. Strong occludin expression is unique to cerebral ECs, probably accounting for the high barrier properties of the blood–brain barrier (BBB).

Tight junctions (TJs) seal the endothelial cell layer and are especially well developed in endothelia of the BBB. This is in contrast to blood vessels outside the CNS, the TJs of which are less elaborate, facilitating exchange of solutes and macromolecules and allowing leucocyte trafficking (Simionescu & Simionescu, 1991). The molecular basis responsible for these different junctional phenotypes and the regulatory mechanisms that control TJs are not yet clear. Two different classes of integral membrane proteins constitute the TJ strands, occludin and members of the claudin protein family (D'Atri & Citi, 2002). Several lines of evidence suggest in this context that the TJ transmembrane protein occludin plays a crucial role in the control of vascular permeability, since tissue expression and content of occludin correlate well with barrier properties (Hirase *et al.* 1997), and overexpression of occludin increases transendothelial electrical resistance in Madin–Darby canine kidney (MDCK) cells (McCarthy *et al.* 1996).

The integrity of the BBB is compromised in many disorders of the human central nervous system (Hatashita & Hoff, 1990; McDonald, 1994). Therapeutic strategies

 DOI: 10.1113/jphysiol.2006.106385

for several of these diseases include treatment with glucocorticoids (GCs; Engelhardt, 2000; Qizilbash *et al.* 2002), but the molecular basis how GCs regulate BBB permeability is not understood. Effects of GCs such as hydrocortisone and dexamethasone are known to be mediated by the glucocorticoid receptor (GR; Beato, 1989). The glucocorticoid receptor can bind to specific DNA sequences (glucocorticoid-responsive element, GRE) in the 5′-flanking region of target genes and so transactivate gene transcription (Beato, 1989).

While barrier-tightening effects of GC treatment have been demonstrated for cerebral endothelial cells, positive effects of GC on peripheral vascular permeability could not be demonstrated clearly. In contrast, side-effects of systemic GC treatment are considerable. Long-term treatment with high levels of GCs causes a range of severe side-effects, such as weight gain concomitant with fat redistribution (Cushing's syndrome), GC-induced hypertension, hyperglycaemia and osteoporosis (Kucharz, 1988; Kimberly, 1991; Canalis *et al.* 2002), so that a further dissection of the molecular events regulating gene transcription at the BBB would be beneficial for the development of target cell-specific GR ligands as therapeutic strategy in the future.

In an attempt to elucidate the molecular mechanisms of GC-induced tightening of the BBB, we were able to show that GC signals can directly act at the transcriptional level by interaction with specific *cis*-acting DNA sequence elements in the occludin gene promoter (Förster *et al.* 2005). In the present study, expression of occludin and GR in BBB and non-BBB (myocardium) endothelial cells was assessed, displaying complete GR downregulation in non-BBB endothelial cells *in vivo* in response to GC treatment. In correlation with these *in vivo* data, divergent target gene promoter transactivating activity of GR in the BBB and non-BBB endothelial cellular context could be demonstrated. We used a model GC-responsive test promoter plasmid after transfection of cell lines generated from brain capillary endothelial cells and the myocardium in the presence and absence of dexamethasone. These data suggest differential signalling mechanisms involved in endothelial barrier regulation between BBB and non-BBB endothelial cells, so that novel brain endothelium-specific ligands for the GR could lead to fine tuning of the transcriptional response of the GR and to circumvention of the side-effects of systemic GC administration.

Methods

Chemicals

Dexamethasone and calpain inhibitor I (LLnL; *N*-acetyl-Leu-Leu-Nle-CHO) were purchased from Sigma, Taufkirchen, Germany.

Animals and collection of tissues

Adult male wild-type mice (6 months old) strain 129 Sv, weighing 30–35 g, were used in the experiments. Mice were maintained under standardized conditions, with free access to food and water. The animals were divided into two experimental groups: saline-treated controls and dexamethasone-treated animals. Animals were treated for 4 days with 10 mg g^{-1} dexamethasone or vehicle alone. Physiological saline and dexamethasone were administered intraperitoneally (I.P.) in a final volume of 250 μl. Mice were killed by CO_2 asphyxiation. Brains and hearts were excised, frozen immediately and stored at −80°C until used for immunohistochemistry and Western blotting, or freeze-dried for immunostaining as described below.

All experiments were approved by the local Animal Care Committee (Tierschutzbeauftragter).

Isolation and culture of cerebral and myocardial vascular endothelial cells

The immortalized mouse brain capillary endothelial cell line cEND was generated as described by Förster *et al.* (2005). Briefly, brains (cerebrum without cerebellum and brainstem) were isolated from neonatal mice (postnatal day 3 mice were killed by decapitation), and, after removal of the meninges and capillary fragments, the tissue was minced in buffer A [15 mM Hepes (pH 7.4), containing 153 mM NaCl, 5.6 mM KCl, 2.3 mM $CaCl_2.2H_2O$, 2.6 mM $MgCl_2.6H_2O$ and 1% (w/v) bovine serum albumin (BSA)] using a sterile cutter. Fragments were digested in 0.75% (w/v) collagenase A (Roche, Mannheim, Germany) for 30 min at 37°C in a water-bath (with occasional shaking). Digestion was stopped by addition of 10 vol. ice-cold buffer A. To remove myelin, centrifugation through a 25% (w/v) BSA gradient was carried out for 20 min at 1000*g*. The resulting endothelial cell pellet was washed twice with buffer A to remove myelin and BSA. Primary cells were then resuspended in Dulbecco's modified Eagle's medium (DMEM; Sigma, Taufkirchen, Germany) growth medium (10% heat-inactivated fetal calf serum) and plated on 24-well plates (Greiner, Frickenhausen, Germany), freshly coated with collagen IV (Fluka, Taufkirchen, Germany) and transfected with Polyoma middle T antiger of murine Polyomavilus (Pym T) (Sabepathy *et al.* 1997) after 24 and after 48 h as previously described for microvascular endothelial cells from brain and heart (Aumailley *et al.* 1991; Golenhofen *et al.* 2002; Förster *et al.* 2005).

The myocardial endothelial cell line MyEnd was generated as described by Golenhofen *et al.* (2002).

Immunostaining

For immunostaining (a) fresh frozen and (b) freeze-dried tissues were used.

(a) Fresh frozen tissues. Small pieces of left ventricular myocardium and brain containing cerebral cortex were frozen in liquid nitrogen-cooled isopentane. Two to 10-μm-thick sections were cut in a cryostat and mounted on glass slides (Superfrost Plus, Menzel). Frozen sections were air dried for 30 min. After washing with ice-cold methanol and acetone, each for 3 min, sections were fixed for 10 min at room temperature in 4% formaldehyde prepared freshly from paraformaldehyde. All sections were treated with 0.1% Triton X-100 in PBS for 5 min, incubated with 10% normal goat serum in PBS for 30 min at 25°C to reduce unspecific binding of secondary antibodies, and exposed in sequence to primary antibodies [rat monoclonal antibody to mouse PECAM-1 (Pharmingen/BD Biosciences, Heidelberg, Germany; 1:100), rabbit polyclonal antioccludin (Zymed Laboratories, CA, USA, zy-*71-1500*; 1:100) and anti-glucocorticoid receptor (Santa Cruz; 1:100) antibodies] and FITC-/ Carbocyarin 3 (Cy3)-conjugated goat anti-rat and goat antirabbit secondary antibodies, respectively. After incubation, coverslips were mounted onto slides using 60% (w/v) glycerol and 1.5% (w/v) *n*-propylgallate (Fluka) as antifading component. The slides were analysed using a Leica TCSSP confocal microscope.

(b) Freeze-dried tissues. Frozen tissue pieces (as described in Fresh frozen tissues section) were freeze dried and embedded in Epon (Serva, Heidelberg, Germany) (Drenckhahn & Franz, 1986). Semithin sections (1 μm) were mounted on glass slides. The resin was removed by placing the slides for 5 min in methanol–toluene (1:1) containing 10% sodium methoxide (prepared from metallic sodium; Mayor *et al.* 1961). All tissue sections were washed at room temperature with PBS, pH 7.4 and then the sections incubated for 24–48 h at 4°C for single and double labelling with the primary anti-bodies diluted into PBS, pH 7.4: anti-PECAM-1, anti-occludin and anti-glucocorticoid receptor, as described above. After several washes with PBS, the sections were incubated for 90 min at room temperature with FITC-/Cy3-labelled secondary antibodies as described above. The sections were examined with a Leica TCSSP confocal microscope.

Optical density measurements (ODs) were carried out on 10 randomly selected vessels from five sections each using Scion Image Beta 4.02 software (Scion Corp., Frederick, MD, USA) to quantify fluorescence. Background fluorescence was eliminated using the subtract background function; for this, control sections were incubated with isotype-specific IgG and primary antibody was omitted and the respective background level subtracted.Since a general increase in fluorescence intensity was observed in sections from dexamethasone-treated animals, the mean increase in FITC-Pecam-1 fluorescence of dexamethasone-treated animals was normalized to the control level before we determined differences in GR or occludin optical density from immunohistochemistry.

Construction of figures

Each single confocal image in a *z*-series captured the distribution of antibody-labelled protein in a 0.5 μm section of the tissue. The *z*-series was then projected to give a single image showing the distribution of the visualized protein in a tissue depth of up to15 μm (see Becker *et al.* 1995 for methods).

Cell cultures

cEND and MyEND cells were cultivated as described above. All cultures were supplemented with 100 IU ml^{-1} penicillin and 100 mg ml^{-1} streptomycin (1% pericillin and steptomicin (PEST)). Cells were maintained in an atmosphere of 5% CO_2−95% O_2 at 37°C.

Electrophoresis and immunoblotting

cEND and MyEND cells were dissolved in Laemmli sample buffer (Laemmli, 1970) and subjected to sodium dodecyl sulphate-polyacrylamide gel electrophoresis (SDS-PAGE, 15% gels). Protein contents were quantified by protein estimation directly from SDS-PAGE loading buffer using 0.1% (w/v) Amidoschwarz (AppliChem, Darmstadt, Germany) in 25% (v/v) methanol−5% (v/v) acetic acid. For immunoblotting, proteins were transferred in Kyhse-Andersen transfer buffer (Kyhse-Andersen, 1984) to Hybond nitrocellulose membranes (Amersham, Braunschweig, Germany) which were blocked with 10% (w/v) low fat milk in PBS (pH 7.4) and incubated overnight at 4°C with the respective primary antibody (in PBS plus 10% low fat milk). The polyclonal rabbit antibodies against occludin and GR were used at a dilution of 1:1000. As secondary antibody, horseradish peroxidase-labelled goat antirabbit IgG (Jackson Immuno Research Laboratory, West Grove, PA, USA) was used diluted 1:3000 with PBS. Bound immunoglobulins were visualized by the enhanced chemiluminescence technique (ECL, Amersham). Densitometric analysis using Scion Image Beta 4.02 (Scion Corp.) was performed for quantification.

Bioelectric and permeability assessments

Cells were plated on top of gelatine-coated transwell chambers for six-well plates (0.4 μm pores; Falcon, Heidelberg, Germany) at densities of 1×10^4 cells per well. When they had reached confluence at day 5, the different experimental sets of cells were transferred to 2% FCS or treated with 100 nM dexamethasone at 2% FCS, respectively. The control set was maintained in basal medium (DMEM, 10% FCS) for an additional

3 days, at which point the permeability measurement was performed. Transendothelial electrical resistance (TER) was measured using an assembly containing current-passing and voltage-measuring electrodes (World Precision Instruments Inc., New Haven, CT, USA). Resistances of blank filters were subtracted from those of filters with cells before final resistances (in $\Omega\,cm^2$) were calculated.

In contrast to cEND cells, MyEND cells were found to partly overgrow in a multilayer structure. To avoid the problem of increased resistance of the endothelial barrier owing to this multilayered structure, MyEnd cells were monitored by light microscopy, and measurements of TER were made where the cells formed a monolayer.

All experiments were repeated at least three times.

Semiquantitative RT-PCR

Total RNA was extracted from confluent cEND and MyEND monolayers after treatment with various differentiation media (for further details see legends to Fig. 4) using the RNeasy Reagent (Quiagen, Hilden, Germany) according to the manufacturer's instructions. RNA was digested with Dnase I (Roche) at 10 units per microgram RNA for 1 h at 37°C followed by heat inactivation for 15 min at 80°C. Two micrograms of total RNA were then reverse transcribed and amplified using the Titan One Tube RT-PCR System (Roche) in a final volume of 50 μl according to the manufacturer's instructions, using 10 mM dNTP (Gibco, Karlsruhe, Germany) and 30 pmol of each primer.

The PCR reactions were performed in a mastercycler gradient thermocycler (Eppendorf) under the following conditions: primers GR forwards (5′-CAA AGC CGT TTC ACT GTC C-3′); GR reverse (5′-ACA ATT TCA CAC TGC CAC C-3′) (Gupta & Wagner, 2003); 94°C for 30 min, 56°C for 30 min, 72°C for 1 min with 35 cycles for each target gene, except in Fig. 4*D*, where 23 cycles were used. A negative control reaction with water as template was included. Glyceraldehyde phosphate dehydrogenase (GAPDH) RNA was used as housekeeping gene. All PCR reactions were done in triplicate for each target.

PCR products were separated on a 1.5% agarose gel stained with ethidium bromide. A 100 bp DNA ladder (Generuler, Fermentas, St. Leon-Rot, Germany) was used for calibration. Band densities were compared under UV transillumination. Densitometric analysis using Scion Image Beta 4.02 (Scion) was performed for quantification.

Claudin-5 quantitative real-time RT-PCR

For real-time RT-PCR, cDNA was synthesized using iSCRIPT cDNA synthesis kit (Bio-Rad) and 1 μg of RNA from cEND or MyEND cells treated or untreated with dexamethasone. Primers were designed using the Primer Express Software (Applied Biosystems) and obtained from MWG Biotech. Real-time RT-PCR was performed using the SYBR®Green PCR Master Mix (Applied Biosystems). Data were acquired with the ABI PRISM 7000 system (Applied Biosystems). Gene expression was normalized to expression of the endogenous housekeeping gene, GAPDH. The mean fold-change in expression of target gene was calculated by using the following equation (where CT means threshold cycle):

$$\Delta CT = CT\ Target - CT\ GAPDH.$$

Transfection and luciferase assay

Essentially, transfection and luciferase assays were carried out as described by Förster *et al.* (2005). Briefly, cEND and MyEND cells were seeded onto a six-well cell culture plate 24 h before transfection in DMEM containing 10% dextran-coated charcoal (DCC)-treated FCS (Fagart *et al.* 1998) and 1% PEST at a density of 2×10^6 cells per well. Transient transfection experiments using the Effectene reagent (Qiagen, Hilden, Germany) were performed as described by the manufacturer, using 2 μg of mouse mammary tumour virus (MMTV; Benore-Parsons *et al.* 1991) and 1 μg of the internal control reporter pTRL-TK (Lorenz *et al.* 1991; Promega) in the absence or presence of ligands (as indicated in the figure legends).

To assess dexamethasone effects on MMTV promoter transactivation, after addition of the DNA–Effectene mixture, cells were incubated overnight at 37°C in 5% CO_2−95% O_2. After this, 4 ml fresh DMEM containing 10% DCC-treated FCS−1% PEST and ligands or vehicle alone (as indicated in the figure legends) were added. After 24 h, cells were washed once with PBS and harvested with 500 μl lysis buffer. Thereafter, cellular extracts were prepared and analysed for luciferase activity. Measurement of both firefly and Renilla luciferase activity was performed with the Dual-Luciferase assay kit (Promega, Madison, WI, USA) according to the manufacturer's instructions. Protein concentration was estimated by standard Bradford protein assay (Bradford, 1976). Cell lysate (20 μl) was used for assaying the enzymatic activities, using a LB9507 luminometer with dual injector (Berthold, Bad Wildbad, Germany). Each lysate was measured twice. Promoter activities were expressed as relative light units (RLU), normalized for the protein content and the activity of Renilla luciferase in each extract. The data were calculated as the mean of five identical set-ups.

Analysis and statistics

Values for TER and induction of luciferase activity were averaged to establish a single value for cEND and MyEND

cells under different experimental conditions. All data are presented as means ± S.E.M. Statistical analysis was performed with analysis of variance (ANOVA) for multiple comparisons and Bonferroni *post hoc* test for statistical significance. Statistical significance was achieved when $P < 0.05$.

Results

Localization of occludin in mouse BBB and non-BBB blood vessels *in vivo*

Using double-labelling immunofluorescence, we examined the level of the TJ protein occludin in endothelial cells of BBB microvessels and in endothelial cells of non-BBB microvessels of the heart in the presence and absence of dexamethasone.

Blood vessels were marked by PECAM-1 staining (green, Fig. 1*A*, *D*, *E* and *H*), an endothelial and platelet marker protein (Newman *et al.* 1990). In brain microvessels from untreated mice, labelling for occludin was consistently detected (red, Fig. 1*B* and *C*). In brains from dexamethasone-treated mice, occludin staining was enhanced, visible as bright fluorescence outlining brain capillaries, which confirmed occludin upregulation by dexamethasone treatment (Fig. 1*F* and *G*). Optical density measurements (ODs) were carried out from five sections each using Scion Image Beta 4.02 software to quantify fluorescence. Background fluorescence was eliminated using the subtract background function. In this way we could demonstrate a 2.04 ± 0.3-fold increase in occludin fluorescence in dexamethasone-treated cerebral vessels.

In blood vessels from the heart of control mice, a different situation was encountered; while the endothelial marker protein PECAM-1 was detected at the plasma membrane (green, Fig. 1*D* and *H*), no occludin staining could be detected (Fig. 1*D*). After dexamethasone treatment, there was no enhancement of occludin signal, while PECAM-1 gave a strong signal (Fig. 1*H*).

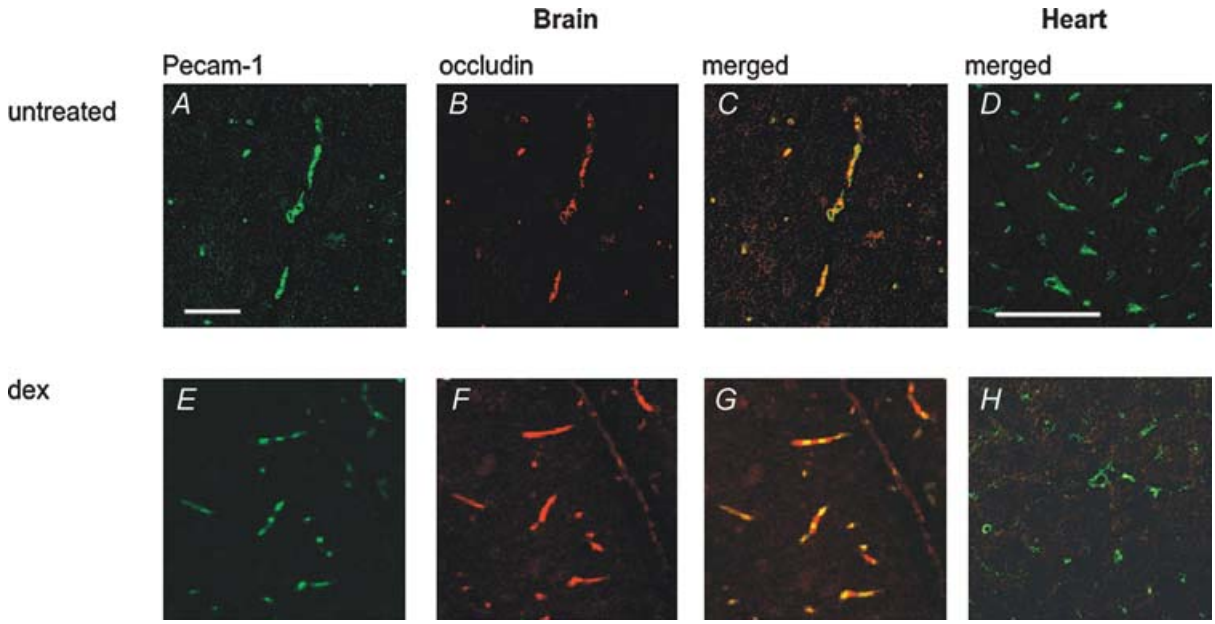

Figure 1. Occludin expression in blood vessels from mouse brain and heart tissue with and without GC treatment

A–C and *E–G* show immunohistochemical detection of occludin (Cy3, red) and PECAM-1 (FITC, green) on freeze-dried brain sections of untreated (*A–C*) and dexamethasone treated mice (*E–G*) on day 4 of treatment with dexamethasone or vehicle. Brain capillaries of untreated mice are positive for both PECAM-1 (green, *A*) and occludin (red, *B*); *C* shows a merged image thereof. Note the increase of occludin immunostaining (red, *F*) in brains of dexamethasone-treated animals; optical density measurements showed a 2.04 ± 0.3-fold increase in occludin fluorescence in dexamethasone-treated cerebral vessels. PECAM-1 labelling is shown in green (*E*). *G* shows a merged image of *E* and *F*. *D* and *H* show immunohistochemical detection of occludin (Cy3, red) and PECAM-1 (FITC, green) on frozen sections from hearts of untreated and dexamethasone-treated mice on day 4 of treatment with dexamethasone or vehicle. *D* and *H* show merged images of representative sections of control (*D*) and dexamethasone-treated hearts (*H*). Microvessels of myocardium lack occludin both in controls (*D*) and after dexamethasone treatment (*H*). The panels are representative for the observations made in all the 3 mice analysed per group. Images were captured using laser scanning confocal microscopy (CLSM). Scale bar in *A* represents 75 μm for *A–C* and *E–G*; scale bar in *D* indicates 50 μm for *D* and *H*.

Localization the GR in mouse BBB and non-BBB endothelial cells with and without dexamethasone treatment

In a murine immortalized brain capillary endothelial cell culture system, which is responsive to GCs (cEND) we recently demonstrated that GCs increase barrier properties of brain capillary endothelial cells by inducing enhanced expression of occludin via binding of the activated glucocorticoid receptor to putative glucocorticoid-responsive elements in the occludin promoter (Förster *et al.* 2005).

In this study, we correlated GR protein contents in BBB and non-BBB microvessels with occludin protein contents *in vivo* and compared these data with *in vitro* data utilizing *in vitro* models of heart and brain capillary endothelial cells (MyEnd, Golenhofen *et al.* 2002; and cEND, Förster *et al.* 2005).

We performed PECAM-1–GR double immunolabelling in brain slices (Fig. 2*A*–*D*). In brain microvessels from control mice identified by PECAM-1 immunoreactivity (Fig. 2*A*), GR protein was weakly detected as cytoplasmic staining by immunohistochemistry (Fig. 2*B*). In constrast, in dexamethasone-treated mice, we observed strong staining for GR protein (Fig. 2*D*). Optical density measurements showed a 2.1 ± 0.2-fold increase in Cy3 GR fluorescence in dexamethasone-treated vessels. We correlated the *in vivo* observations with *in vitro* data. In untreated cEND cells, weak GR immunofluorescence (green) could be detected in the cytoplasmic compartment (Fig. 3*A* and *B*). Upon dexamethasone treatment, nuclear concentration of GR was confirmed, visualized by propidium iodide nuclear counterstaining (red, Fig. 3*C* and *D*). After dexamethasone treatment, fluorescence was concentrated to the nucleus in cEND cells, as confirmed by the use of computer imaging software (Adobe Photoshop CS, Seattle, WA, USA) to merge the individual images for FITC–GR and propidium iodide counterstain to assess similarity of staining pattern. However, a $38 \pm 0.6\%$ reduction of total optical density over the full cellular area was estimated in cEND cells.

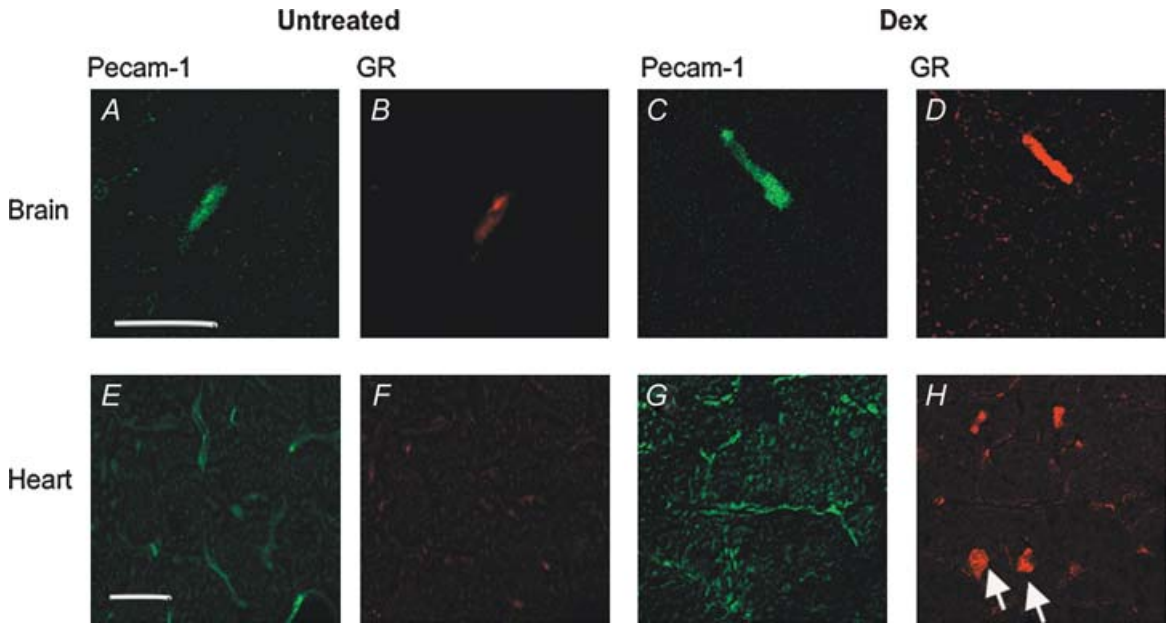

Figure 2. Confocal fluorescence microscopy depicting GR localization in blood vessels from brain and heart with and without dexamethasone treatment
A–D show immunohistochemical detection of GR (Cy3, red) and PECAM-1 (FITC, green) on freeze-dried sections from cerebral cortex. Panels show representative sections of control (*A* and *B*) and dexamethasone-treated mouse brains (*C* and *D*) on day 4 of treatment, stained for PECAM-1 (*A* and *C*) and GR (*B* and *D*), respectively. Note the strong enhancement of GR immunosignal within dexamethasone-treated endothelial cells of the BBB (*D*). A 2.1 ± 0.2-fold increase in Cy3 GR fluorescence could be observed in dexamethasone-treated vessels as assessed by optical density measurements. Scale bar in *A* represents 20 μm for *A–D*. *E–H* show double immunofluorescence labelling of heart cryosections of untreated (*E* and *F*) and dexamethasone-treated mice (*G* and *H*) on day 6 of treatment with dexamethasone or vehicle. Endothelial cells are visualized by PECAM-1 immunostaining (FITC; *E* and *G*), GR localization by Cy3-coupled antibody labelling (*F* and *H*). In contrast to observations on the brain, GR protein could not be detected in heart endothelial cells either in control mice or in dexamethasone-treated animals by immunohistochemistry using flourencence-labelled antibody. However, dexamethasone treatment caused strong GR nuclear staining in cardiomyocytes (arrows in *H*). Scale bar in *E* respresents 20 μm for *E–H*.

This observation was in sharp contrast to the situation in non-BBB blood vessels from the heart and in MyEND cells. PECAM-1 immunoreactivity was very conspiciuous in endothelium of the heart (Fig. 2*E*) in untreated mice. Glucocorticoid receptor immunoreactivity was below the detection limit by immunohistochemistry in endothelial cells of the heart (Fig. 2*F*) of untreated mice. In contrast to the BBB, in blood vessels from the heart of dexamethasone-treated mice, GR protein was not increased in endothelial cells, whereas strong nuclear GR staining of cardiomyocytes was observed in response to dexamethasone treatment (arrows, Fig. 2*H*).

Correspondingly, in untreated MyEND cells, very faint immunofluorescence (green) could be detected in the cytoplasmic compartment (Fig. 3*E* and *F*). Pixel analysis for the different levels of FITC fluorescence showed that control MyEND cells did express a 2.9 ± 0.2-fold lower staining density for FITC–GR than control cEND cells.

After dexamethasone treatment, optical density measurement showed a $42 \pm 0.3\%$ reduction of total optical density of GR immunosignal over the full cellular area. No nuclear concentration of GR (green) could be detected in MyEND cells upon dexamethasone treatment, visualized by propidium iodide nuclear counterstaining (red, Fig. 3*G* and *H*).

Correlation of *in vivo* and *in vitro* data on endothelial cell permeability

We examined the expression of occludin and claudin-5 protein in the presence and absence of dexamethasone in cEND and MyEND cells. After dexamethasone treatment, we observed a 2.4 ± 0.3-fold increase ($n = 3$) in occludin levels in cEND cells, as determined by densitometric analysis of Western blots (Fig. 4*A*), while

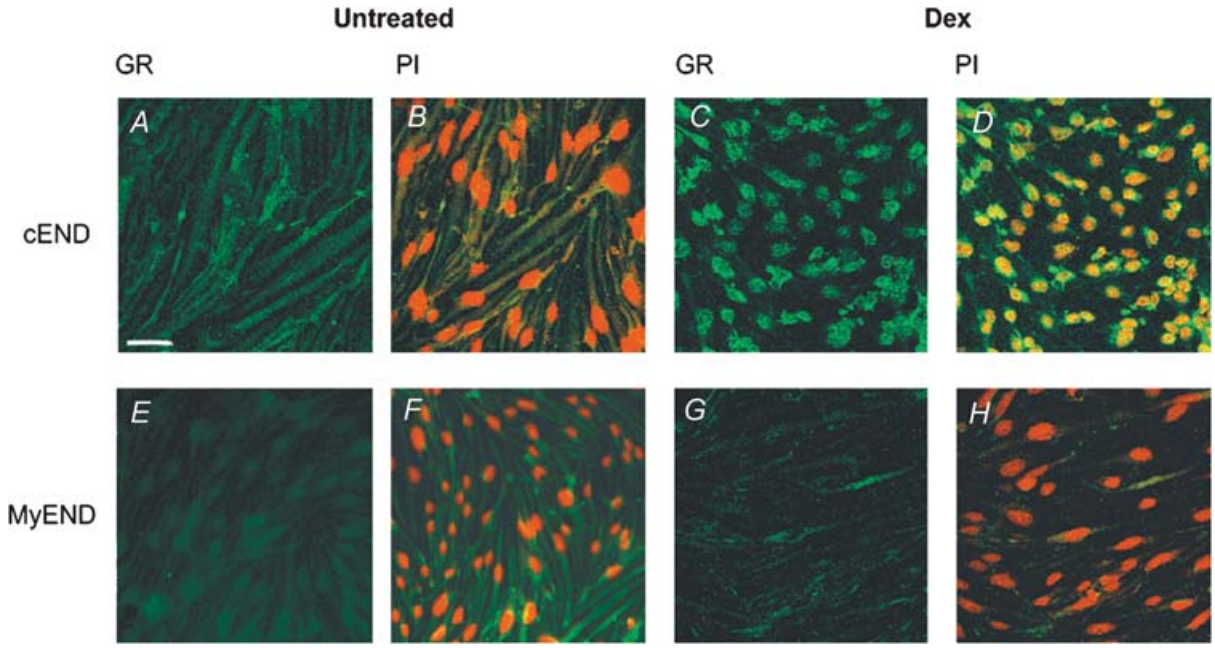

Figure 3. Glucocorticoid receptor protein in cEND brain capillary endothelial cells and MyEND non-BBB endothelial cells
A–D, immunocytochemistry visualizing GR protein (FITC, green) in cEND brain capillary control endothelial cells (*A*) and after treament with 100 nM dexamethasone (*C*). *B* and *D* represent merged images of GR immunofluorescence (green), and nuclei are counterstained by propium iodide (red) in control (*B*) and dexamethasone-treated cEND cells (*D*). Untreated cEND cells expressed a 2.9 ± 0.2-fold higher staining density for FITC GR than untreated MyEND cells. After dexamethasone treatment, a $38 \pm 0.6\%$ reduction of total optical density over the full cellular area occurred in cEND cells. The nuclear concentration of GR could be confirmed for dexamethasone-treated cEND cells by the use of computer imaging software to merge the individual images for FITC GR and propidium iodide counterstain to assess the similarity of staining pattern. *E–H*, immunocytochemistry visualizing GR protein (FITC, green) in control MyEND endothelial cells (*E*) and after treatment with 100 nM dexamethasone (*G*). *F* and *H* represent merged images of GR immunofluorescence (green), and nuclei are counterstained by propium iodide (red) in control (*F*) and dexamethasone-treated cEND cells (*H*). Optical density measurement showed that a $42 \pm 0.3\%$ reduction of total optical density over the full cellular area occurred in MyEND cells after dexamethasone treatment. In accordance with the *in vivo* situation, no nuclear concentration of GR (green) could be detected in MyEND cells upon dexamethasone treatment, visualized by propidium iodide nuclear counterstaining (red). Images were captured using laser scanning confocal microscopy. Scale bar in *A* represents 45 μm.

levels of claudin-5 were unaffected (Fig. 4*B*). In contrast, there was no occludin protein detectable by immunoblotting in the myocardial cell line, MyEND, under control conditions (Fig. 4*C*). Serum reduction and dexamethasone administration did not lead to a detectable upregulation of occludin protein (Fig. 4*C*). Basal claudin-5 protein levels were 2 ± 0.2-fold higher in cEND cells than in MyEND cells, as evaluated by densitometric analysis.

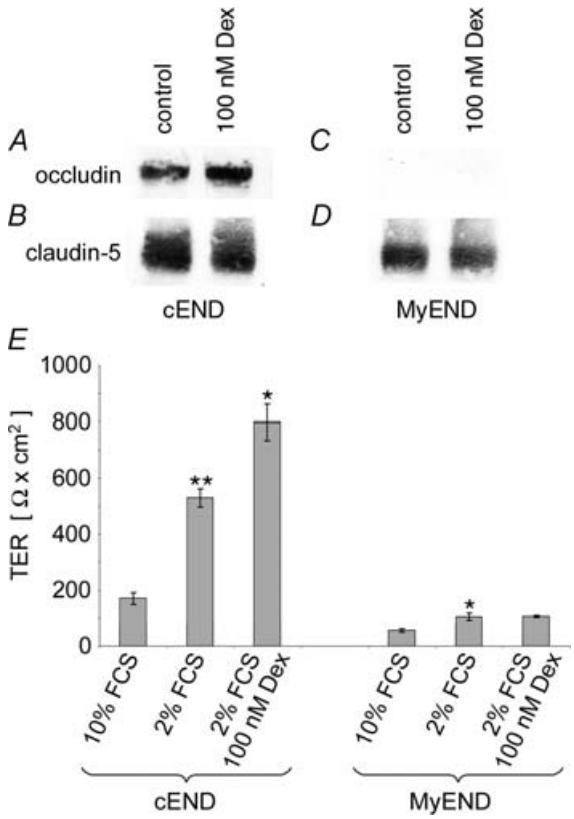

Figure 4. Dexamethasone effects on TER and on occludin and claudin-5 protein levels in cEND and MyEnd endothelial cells
Confluent monolayers of cEND and MyEnd cells were grown in gelatine-coated cell culture flasks in the presence or absence of 100 nM dexamethasone for 24 h. Cell lysates were analysed by Western blot for occludin and claudin-5. Densitometric evaluation resulted in an 2.4 ± 0.3-fold ($n = 3$) upregulation of occludin protein content in cEnd cells in the presence of dexamethasone (*A*), while claudin-5 protein levels remained unaffected (*B*). Occludin could not be detected in MyEND cells (*C*), while claudin-5 protein levels were also uneffected (*D*). Note the different basal (occludin) and claudin-5 protein levels in control cEnd and MyEnd cells (*A* and *C*). *E*, influence of serum reduction and the addition of dexamethasone on the electrical barrier properties (TER) of cEND and MyEND monolayers. Growth medium (10% FCS) was changed after 5 days in culture to differentiation medium (2% FCS, with or without additions), and analysis of the TER was performed after 7 days *in vitro*. Incubation medium: 10% (v/v) FCS, without dexamethasone (dex); 2% (v/v) FCS, without dexamethasone; 2% (v/v) FCS, 100 nM dexamethasone. Data are given as means ± S.D. ($n = 6$). The values were compared through analysis of variance (ANOVA) with Bonferroni *post hoc* test: P values < 0.05 were considered significant (*) and P values < 0.005 were considered highly significant (**).

As in cEND cells, claudin-5 levels in MyEND cells were unaffected by dexamethasone treatment, indicating that claudin-5 is not regulated by GCs in either endothelial cell line (Fig. 4*D*). We confirmed the insensitivity of the claudin-5 gene to dexamethasone at the transcriptional level by using quantitative real-time RT-PCR to compare expression levels of claudin-5 in cEND and MyEND cells grown in medium supplemented with 10% serum or 2% serum or 2% serum plus dexamethasone. The level of claudin-5 mRNA was comparably high in both cell lines. However, no significant changes in claudin-5 expression could be observed after serum reduction or additional treatment with dexamethasone (results not shown), supporting the observations made at the protein level.

High occludin and claudin-5 protein levels could account for high transendothelial electrical resistance of brain capillary endothelial cells as opposed to non-BBB cells (Fig. 4*E*). In the presence of 10% serum contained in the growth medium, TER of cEND cells was about $170 \pm 20\ \Omega\ cm^2$. Reduction of serum to 2% resulted in a significant increase of TER to the range of $500 \pm 50\ \Omega\ cm^2$ in cEND cells. The addition of saturable concentrations of dexamethasone (EC_{50} for maximal transactivating effects of dexamethasone $= 10^{-8}$ M; Jaffuel *et al.* 2001) to the serum-reduced endothelial differentiation medium induced a further significant increase of TER up to $800 \pm 80\ \Omega\ cm^2$ (Fig. 4*E*). In contrast, in MyEND cells, TER was estimated to represent about $105 \pm 14\ \Omega\ cm^2$ in endothelial differentiation medium (2% FCS), while we measured $55 \pm 6\ \Omega\ cm^2$ in high serum (10% FCS) medium (Fig. 4*E*). In contrast to cEND cells, however, in MyEND cells, dexamethasone administration did not cause a further elevation of TER ($106 \pm 4\ \Omega\ cm^2$).

Tissue-specific transactivation activity of GR in endothelial cells from different vascular beds

In an effort to explain the differences in the GC sensitivity of cEND cells as opposed to MyEND cells, we examined GR expression in these cell lines by Western blot and tested transactivation activity of GR in the endothelial cellular context in the presence and absence of dexamethasone (Fig. 5). In cell lysates from control cEND cells, there was a strong signal for GR protein detectable. Dexamethasone treatment led to $50 \pm 6\%$ reduction in detectable GR protein ($n = 3$; Fig. 5*A*) concomitant with receptor translocation to the nucleus (Fig. 3*C* and *D*).

Control MyEND cells contained $24 \pm 3\%$ of the amount of GR protein detected in control BBB cEND cells, as evaluated by densitometric analysis of Western blots. By 12 h of dexamethasone treatment, downregulation of GR protein to the detection limit, an estimated protein content of $40 \pm 6\%$ of the untreated MyEND cells, occurred ($n = 3$; Fig. 5*A*). Further investigation showed

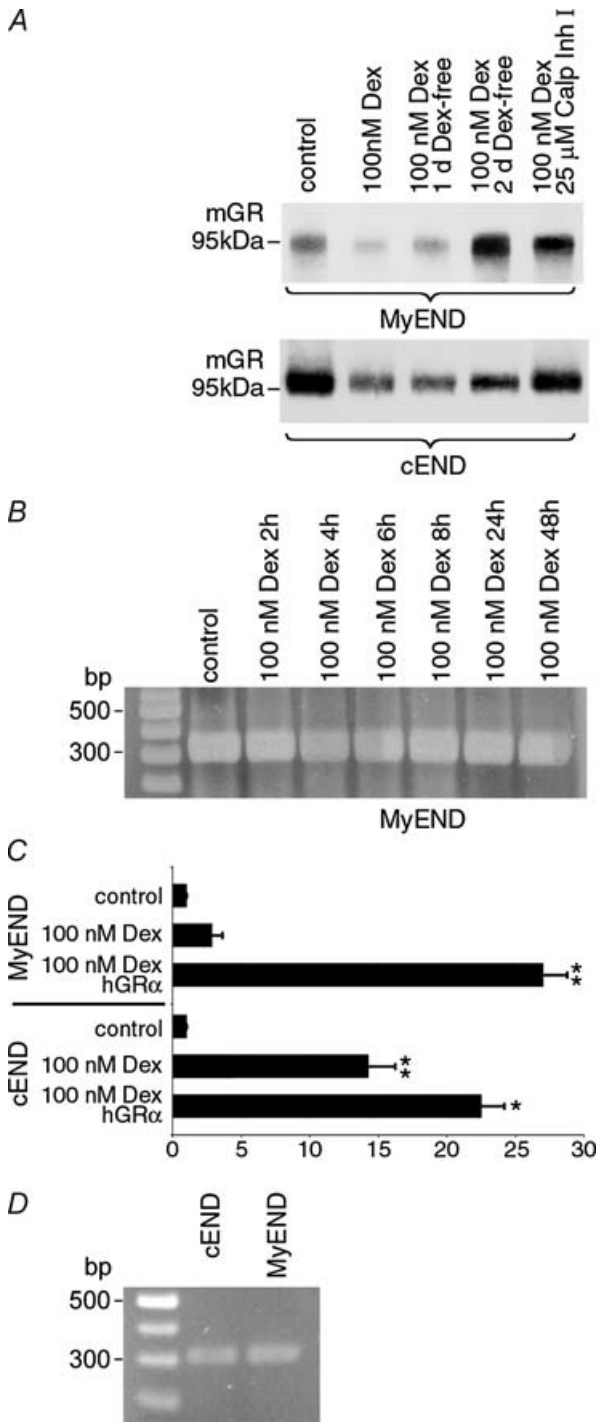

Figure 5. Dexamethasone administration leads to strong downregulation of GR protein and loss of transcriptional activation on GR target genes in peripheral endothelial cells
A, confluent monolayers of cEND and MyEnd cells were grown in gelatine-coated cell culture flasks in the presence of 100 nM dexamethasone and 25 μM calpain inhibitor I as indicated. Cell lysates were analysed by Western blot for GR protein. Control MyEND cells contained $24 \pm 3\%$ of the amount of GR protein detected in control BBB cEND cells as evaluated by densitometric analysis of Western blots. By 12 h of dexamethasone treatment, downregulation of GR protein to the detection limit, an estimated protein content of $40 \pm 6\%$ of the untreated cells, occurred ($n = 3$), while a reduction to $38 \pm 3\%$ occurred in the BBB cell line cEND. Receptor downregulation at the protein level could be reversed by dexamethasone withdrawal for 1–2 days, now representing $70 \pm 5\%$ and $120 \pm 12\%$ of the untreated cells, respectively, or inhbition of the 26S proteasome by calpain inhibitor I (Calp Inh I) during dexamethasone treatment in MyEND cells. In cEND cells, ligand-dependent GR protein downregulation was also counteracted by calpain inhibitor I or reversed by dexamethasone withdrawal (reappearance to $45 \pm 5\%$ and $80 \pm 8\%$ of untreated cells after 1 or 2 days, respectively, without dexamethasone). *B*, after reaching confluence, MyEND cells were treated with 100 nM dexamethasone (Dex) for up to 2 days, and mRNA expression was assessed at defined time points. No difference in GR mRNA expression was observed over the duration of the experiment. *C*, cEND and MyEND cells were cotransfected with reporters pMMTV-luc (Benore-Parsons *et al.*, 1991) and pRL-TK (Promega), then grown with or without 100 nM dexamethasone as indicated for 24 h. Cell extracts were assayed for Luc and Renilla activity. As a positive control, for both cell types a set of data showing transactivation after cotransfection with hGRα was included. The transactivation activity without dexamethasone was considered as the baseline activity of the promoter. The results are displayed as the ratio of activity with ligands to activity without (mean and S.D. from at least 4 experiments). In cEND cells, MMTV promoter is transactivated 14 ± 2.1-fold ($n = 4$) by endogenous GR in the presence of dexamethasone, but very little transactivation by GR (3 ± 1.7-fold) could be demonstrated in MyEND cells, thus mimicking the situation observed *in vivo* in non-BBB cells. Cotransfection of hGRα resulted in 22 ± 1.73-fold transactivation in cEND and 27 ± 1.76-fold transactivation in MyEND cells. Values were compared through analysis of variance (ANOVA) with Bonferroni *post hoc* test: P values < 0.05 were considered significant (*) and P values < 0.005 were considered highly significant (**). *D*, after reaching confluence, GR mRNA expression was compared in control cEND and MyEND cells. No difference in GR mRNA expression was observed between the two cell lines.

that dexamethasone did not cause a reduction of GR in cells treated with calpain inhibitor I, a specific inhibitor of the 26S proteasome (Fang *et al.* 1998; Fig. 5*A*). Likewise, medium replacement and dexamethasone withdrawal for 1 or 2 days after dexamethasone treatment led to reappearance of GR protein to levels which amount to $70 \pm 5\%$ and $120 \pm 12\%$, of the levels observed in the untreated MyEND cells (Fig. 5*A*). In contrast to downregulation of GR protein, RT-PCR analysis clearly showed that there was no downregulation of GR transcript by dexamethasone during 2 days of treatment in MyEND cells (Fig. 5*B*). A comparable protein downregulatory effect of dexamethasone treatment (to levels which amount to $38 \pm 3\%$ of the levels observed in untreated cells) was observed in cEND cells, which could also be counteracted by calpain inhibitor I or reversed by dexamethasone withdrawal (reappearance to 45 ± 5 and $80 \pm 8\%$ in untreated cells after 1 or 2 days, respectively, without dexamethasone; Fig. 5*A*).

Summarizing protein expression data collected by Western blot analysis and immunocytochemistry, we show that ligand-bound GR is: (a) partly degraded and partly translocated to the nucleus in BBB endothelial cells; and (b) degraded to the detection limit in non-BBB endothelial cells.

Low contents in GR protein were hypothesized to account for the lack of GC sensitivity of MyEND cells compared with cEND cells. To test GR transactivation activity in the BBB and non-BBB endothelial cells, the model MMTV test promoter, which contains five classical consensus GREs (5′-GTTACAnnnTGTTCT-3′; Benore-Parsons *et al.* 1991) was introduced into cEND and MyEND cells. To this end, both endothelial cell lines were cotransfected with the promoter–reporter construct pMMTV-luc (Benore-Parsons *et al.* 1991) and pRL-TK (Promega), then grown with or without 100 nM dexamethasone as indicated for 24 h. Cell extracts were assayed for Luc and Renilla activity (Fig. 5*C*). As a positive control, for both cell types a set of data showing transactivation after cotransfection with human glucocorticoid receptor alpha (hGRα) was included. The transactivation activity without dexamethasone was considered as the baseline activity of the promoter. The results are displayed as the ratio of activity with ligands to activity without (mean and S.D. from at least 4 experiments). While in cEND cells, MMTV promoter is transactivated 14 ± 2.1-fold ($n = 4$) by endogenous GR (Fig. 5*C*), very litlle transactivation by GR (3 ± 1.7-fold) could be demonstrated in MyEND cells (Fig. 5*C*), which demonstrates cell-specific differences between endothelial cell subtypes in the GR transactivation function upon binding with dexamethasone. Cotransfection of hGRα resulted in 22 ± 1.73-fold transactivation in cEND and 27 ± 1.76-fold transactivation in MyEND cells.

Discussion

Glucocorticoids play a pivotal role in the clinical management of CNS diseases with impaired BBB function, e.g. brain oedema or brain tumours (Kaal & Vecht, 2004). Furthermore, they play an important role in the treatment of neuro-oncologic diseases (Koehler, 1995) and acute ischaemic stroke (Qizilbash *et al.* 2002). The introduction of corticosteroid therapy in the early 1960s coincided with a remarkable decline in perioperative mortality rates and indicates the importance of these drugs (Kaal & Vecht, 2004). The oedema-reducing effect of corticosteroids is rapid. Reductions in capillary permeability are observed within a few hours after a single dose of a corticosteroid; however, the underlying molecular mechanisms are not clear. Recent studies have begun to indicate that corticosteroids reduce expression of the oedema-producing factor vascular endothelial growth factor (VEGF), which signals towards endothelial cell dedifferentiation, thus pointing to a role for GC signalling in endothelial cell differentiation (reviewed by Kaal & Vecht, 2004). Dexamethasone is the most commonly used corticosteroid. It is 30 times as potent as cortisol, the endogenous GC present in the bloodstream, and approximately six times as potent as, for example, prednisolone. Dexamethasone reaches full effect within 24–72 h. Interestingly, therapeutic GC effects correlate well with the pathophysiological observation that there is a significant increase of the endogenous cortisol concentration in plasma and cerebrospinal fluid in patients with brain ischaemia, potentially a part of the body's self-repair response to tissue damage (Selakovic, 2004).

However, adverse side-effects of chronic GC administration and afflictions such as gastrointestinal haemorrhage in acute treatment prevail, so that the 'ideal' agent for the treatment of BBB dysfunction remains to be discovered. The development of brain endothelium-specific GR ligands seems further indicated by the fact that, in contrast to beneficial effects of GCs on the brain endothelium, no protection for endothelium of the heart could be observed in many clinical trials (da-Luz *et al.* 1982; Madias & Hood, 1982; Shatney & Lillehei, 1982; LeGal & Morrissey, 1990). Rather, multifactorial indications for the pathogenesis of GC-induced hypertension are given (reviewed by Saruta, 1996).

As a basis for the development of tissue-specific GR ligands, we considered it appropriate to examine GR receptor status and GC responsivity in BBB and non-BBB endothelial cells. It is well recognized that the principal functions of the endothelium (the control of haemostasis, vasomotor tone, cell and nutrient trafficking, barrier function and angiogenesis) are differentially regulated between different sites of the vascular tree and from one moment to the next (reviewed by Aird, 2003). The structural peculiarities of intercellular junctions are, for instance, considered to account for the differences in permeability displayed by various vascular beds; strong occludin expression is unique to cerebral ECs, probably accounting for the permeabilty properties of the BBB (reviewed by Feldman *et al.* 2005). Disruption of occludin staining patterns of BBB endothelia is a hallmark of miscellaneous diseases (reviewed by Feldman *et al.* 2005). Finally, ageing itself has been linked to declining occludin content in BBB endothelial cells (Mooradian *et al.* 2003). Our data show, in accordance with previous observations (Vorbrodt & Dobrogowska, 2003), a high concentration of immunosignal for occludin in BBB-type brain capillaries. In non-BBB-type capillaries which supply the mouse heart, the majority of interendothelial junctions remain weakly immunolabelled or unlabelled. Our data are thus consistent with the findings of other authors, who, using immunofluorescence microscopy and electron microscopy, observed a high expresssion of occludin in brain capillaries and only negligible expression in some non-BBB vascular profiles, e.g. in the heart (Furuse *et al.* 1993).

In a murine immortalized brain capillary endothelial cell culture system, which is responsive to GCs (cEND), we recently demonstrated that GCs increase barrier properties

of brain capillary endothelial cells by inducing enhanced expression of the TJ transmembrane protein occludin via binding of the activated GR to putative GC-responsive elements in the occludin promoter (Förster *et al.* 2005).

Generally, the nature and magnitude of the response of a cell to glucocorticoids are dependent on the hormone levels it is exposed to as well as the intracellular concentration of receptor, in additon to the efficiency of GR-mediated signal transduction, and the genomic accessibility of glucorticoid-responsive genes (reviewed by Zhou & Cidlowski, 2005). In the present study, we tried to correlate endothelial barrier function (manifested by occludin expression) with the GR status of endothelial cells of the BBB and of non-BBB endothelial cells *in vivo* and *in vitro*, using endothelial cells from the BBB (cEND) and the myocardium (MyEND). We showed enhancement of occludin fluorescence intensity after dexamethasone administration exclusively at the BBB *in vivo* and *in vitro*, consistent with our previous observations in cEND cells (Förster *et al.* 2005). Results further demonstrated that GR receptor status and glucocorticoid responsivity do differ between endothelial cells from various vascular beds (BBB and heart), thus proving biochemical and endocrine heterogeneity. Our data showed that ligand-bound GR is: (a) partly degraded and partly translocated to the nucleus in BBB endothelial cells; and (b) degraded to the detection limit in non-BBB endothelial cells.

This result was validated by testing the transactivating activity of GR in the endothelial cellular context in the presence and absence of dexamethasone on the model MMTV test promoter, which contains five consensus GREs (Benore-Parsons *et al.* 1991). Glucocorticoid responsivity could thereby only be demonstrated for endothelial cells of the BBB, which was attributed to very low GR protein levels in non-BBB endothelial cells, which experienced a complete downregulation upon dexamethasone treatment.

Biochemical studies elucidated that ligand-dependent (dexamethasone) downregulation of mature GR occurs at the protein level in endothelial cells irrespective of their origin by a mechanism involving destruction by the 26S proteasome. Calpain inhibitor I, a specific inhibitor of the 26S proteasome, blocked dexamethasone-induced downregulation. Calpain executes limited proteolysis of its own substrates and is considered a modulator of various intracellular signalling pathways (Huang & Wang, 2001). Hormone-dependent downregulation of a related steroid receptor, progesterone receptor (PR), has been demonstrated in the past in other tissues (Lange *et al.* 2000). For the GR, tissue-specific expression has been demonstrated solely on the level of transcription so far. Glucocorticoid receptor mRNA was greatest in the lung, with the relative levels in other tissues as follows: spleen, 70%; brain, 55%; liver, 50%; kidney, 43%; heart, 35%; and adrenal, 13% (Kalinyak *et al.* 1987).

The biological significance of ligand-dependent downregulation of nuclear receptors at the post-transcriptional level has been discussed. One reason for clearance of activated protein might be to attenuate transcriptional responses in a tissue-specific manner in tissues continually activated by ligand (Shen *et al.* 2001), a situation occurring precisely in the blood vessel-lining endothelial cells.

Differences in GR levels between endothelial cells from various vascular beds has, however, not been assessed so far. We take this approach one step further and prove endothelium-specific regulation of GR protein. We demonstrate differrent GR protein contents in endothelial cells from various vascular beds. As discussed above, ligand-binding leads to hormone-dependent downregulation of GR protein in both BBB and non-BBB endothelial cells, but the resulting GC response differs; while GR activation and translocation occurs in BBB endothelial cells, non-BBB endothelial cells appear to lose GC responsivity. By comparison of GR contents in untreated and dexamethasone-treated cells, we could attribute this to different basal amounts of GR protein in BBB and non-BBB endothelial cells, probably resulting from different protein stability of the unliganded receptor in BBB and non-BBB endothelial cells. However, the underlying mechanism leading to stabilization of the unliganded GR, which impedes its degradation by the proteasome and extends receptor half-life in BBB endothelial cells, remains to be elucidated. One possible explanation could be the action of GR-interacting proteins to stabilize the GR in the absence of ligands, which has been demonstrated previously (Ismaili *et al.* 2005).

Taken together, our data provide for the first time mechanistic insight into GR content and regulation within endothelial cell populations from various vascular beds. Our *in vitro* data obtained from the immortalized cell lines cEND and MyEND reflect the *in vivo* situation well, thereby validating them as a useful model system for BBB and non-BBB endothelial cells. These observations and the model systems used thus appear well suited to provide a basis to open up a new lead for the development of GR agonists that selectively activate specific signal transduction pathways towards brain capillary endothelial cell differentiation as novel weapons to combat BBB dysfunction. In contrast, our data might form the basis for the molecular analyses of events leading to GC-induced hypertension, which might be caused by the loss of potential vasoprotective GR function under dexamethasone treatment.

References

Aird WC (2003). Endothelial cell heterogeneity. *Crit Care Med* **31**, S221–S230.

Aumailley M, Timpl R & Risau W (1991). Differences in laminin fragment interactions of normal and transformed endothelial cells. *Exp Cell Res* **196**, 177–183.

Beato M (1989). Gene regulation by steroid hormones. *Cell* **56**, 335–344.

Becker DL, Evans WH, Green CR & Warner A (1995). Functional analysis of amino acid sequences in connexin43 involved in intercellular communication through gap junctions. *J Cell Sci* **108**, 1455–1467.

Benore-Parsons M, Liebman J & Wennogle LP (1991). Binding of glucocorticoid receptors to model DNA response elements. *J Cell Biochem* **47**, 330–336.

Bradford MM (1976). A rapid and sensitive method for the quantitation of microgram quantities of protein utilizing the principle of protein-dye binding. *Anal Biochem* **72**, 248–254.

Canalis E, Pereira RC & Delany AM (2002). Effects of glucocorticoids on the skeleton. *J Pediatr Endocrinol Metab* **15**(Suppl. 5), 1341–1345.

da-Luz PL, Leite JJ, Barros LF, Dias-Neto A, Zanarco EL & Pileggi FJ (1982). Experimental myocardial infarction: effect of methylprednisolone on myocardial blood flow after reperfusion. *Braz J Med Biol Res* **15**, 355–360.

D'Atri F & Citi S (2002). Molecular complexity of vertebrate tight junctions. *Mol Membr Biol* **19**, 103–112.

Drenckhahn D & Franz H (1986). Identification of actin-, α-actinin-, and vinculin-containing plaques at the lateral membrane of epithelial cells. *J Cell Biol* **102**, 1843–1852.

Engelhardt B (2000). Role of glucocorticoids on T cell recruitment across the blood–brain barrier. *Z Rheumatol* **59**(Suppl. 2), II/18–II/21.

Fagart J, Wurtz JM, Souque A, Hellal-Levy C, Moras D & Rafestin-Oblin ME (1998). Antagonism in the human mineralocorticoid receptor. *EMBO J* **17**, 3317–3325.

Fang CH, Wang JJ, Hobler S, Li BG, Fischer JE & Hasselgren PO (1998). Proteasome blockers inhibit protein breakdown in skeletal muscle after burn injury in rats. *Clin Sci (Lond)* **95**, 225–233.

Feldman GJ, Mullin JM & Ryan MP (2005). Occludin: structure, function and regulation. *Adv Drug Deliv Rev* **57**, 883–917.

Förster C, Silwedel C, Golenhofen N, Burek M, Kietz S, Mankertz J & Drenckhahn D (2005). Occludin as direct target for glucocorticoid-induced improvement of blood–brain barrier properties in a murine *in vitro* system. *J Physiol* **565**, 475–486.

Furuse M, Hirase T, Itoh M, Nagafuchi A, Yonemura S & Tsukita S (1993). Occludin: a novel integral membrane protein localizing at tight junctions. *J Cell Biol* **123**, 1777–1788.

Ghitescu L & Robert M (2002). Diversity in unity: the biochemical composition of the endothelial cell surface varies between the vascular beds. *Microsc Res Tech* **57**, 381–389.

Golenhofen N, Ness W, Wawrousek EF & Drenckhahn D (2002). Expression and induction of the stress protein α-B-crystallin in vascular endothelial cells. *Histochem Cell Biol* **117**, 203–209.

Gupta V & Wagner BJ (2003). Expression of the functional glucocorticoid receptor in mouse and human lens epithelial cells. *Invest Ophthalmol Vis Sci* **44**, 2041–2046.

Hatashita S & Hoff JT (1990). Brain edema and cerebrovascular permeability during cerebral ischemia in rats. *Stroke* **21**, 582–588.

Hirase T, Staddon J, Saitou M, Ando-Akatsuka Y, Itoh M, Furuse M, Fujimoto K, Tsukita S & Rubin L (1997). Occludin as a possible determinant of tight junction permeability in endothelial cells. *J Cell Sci* **110**, 1603–1613.

Huang Y & Wang KK (2001). The calpain family and human disease. *Trends Mol Med* **7**, 355–362.

Ismaili N, Blind R & Garabedian MJ (2005). Stabilization of the unliganded glucocorticoid receptor by TSG101. *J Biol Chem* **280**, 11120–11126.

Jaffuel D, Roumestan C, Balaguer P, Henriquet C, Gougat C, Bousquet J, Demoly P & Mathieu M (2001). Correlation between different gene expression assays designed to measure trans-activation potencies of systemic glucocorticoids. *Steroids* **66**, 597–604.

Kaal EC & Vecht CJ (2004). The management of brain edema in brain tumors. *Curr Opin Oncol* **16**, 593–600.

Kalinyak JE, Dorin RI, Hoffman AR & Perlman AJ (1987). Tissue-specific regulation of glucocorticoid receptor mRNA by dexamethasone. *J Biol Chem* **262**, 10441–10444.

Kimberly RP (1991). Mechanisms of action, dosage schedules, and side effects of steroid therapy. *Curr Opin Rheumatol* **3**, 373–379.

Koehler PJ (1995). Use of corticosteroids in neuro-oncology. *Anticancer Drugs* **6**, 19–33.

Kucharz EJ (1988). Hormonal control of collagen metabolism. Part II. *Endocrinologie* **26**, 229–237.

Kyhse-Andersen J (1984). Electroblotting of multiple gels: a simple apparatus without buffer tank for rapid transfer of proteins from polyacrylamide to nitrocellulose. *J Biochem Biophys Meth* **10**, 203–209.

Laemmli UK (1970). Cleavage of structural proteins during the assembly of the head of bacteriophage T4. *Nature* **227**, 680–685.

Lange CA, Shen T & Horwitz KB (2000). Phosphorylation of human progesterone receptors at serine-294 by mitogen-activated protein kinase signals their degradation by the 26S proteasome. *Proc Natl Acad Sci U S A* **97**, 1032–1037.

LeGal YM & Morrissey LL (1990). Methylprednisolone interventions in myocardial infarction: a controversial subject. *Can J Cardiol* **6**, 405–410.

Lorenz WW, McCann RO, Longiaru M & Cormier MJ (1991). Isolation and expression of a cDNA encoding *Renilla reniformis* luciferase. *Proc Natl Acad Sci U S A* **88**, 4438–4442.

McCarthy KM, Skare IB, Stankewich MC, Furuse M, Tsukita S, Rogers RA, Lynch RD & Schneeberger EE (1996). Occludin is a functional component of the tight junction. *J Cell Sci* **109**, 2287–2298.

McDonald WI (1994). Rachelle Fishman–Matthew Moore Lecture. The pathological and clinical dynamics of multiple sclerosis. *J Neuropathol Exp Neurol* **53**, 338–343.

Madias JE & Hood WB Jr (1982). Effects of methylprednisolone on the ischemic damage in patients with acute myocardial infarction. *Circulation* **65**, 1106–1113.

Mayor HD, Hampton JC & Rosario B (1961). A simple method for removing the resin from epoxy-embedded tissue. *J Biophys Biochem Cytol* **9**, 909–910.

Mooradian AD, Haas MJ & Chehade JM (2003). Age-related changes in rat cerebral occludin and zonula occludens-1 (ZO-1). *Mech Ageing Dev* **124**, 143–146.

Newman PJ, Berndt MC, Gorski J, White GC II, Lyman S, Paddock C & Muller WA (1990). PECAM-1 (CD31) cloning and relation to adhesion molecules of the immunoglobulin gene superfamily. *Science* **247**, 1219–1222.

Qizilbash N, Lewington SL & Lopez-Arrieta JM (2002). Corticosteroids for acute ischaemic stroke. Cochrane Database Syst Rev, CD000064.

Sabapathy KT, Pepper MS, Kiefer F, Mohle-Steinlein U, Tacchini-Cottier F, Fetka I, Breier G, Risau W, Carmeliet P, Montesano R & Wagner EF (1997). Polyoma middle T-induced vascular tumor formation: the role of the plasminogen activator/plasmin system. *J Cell Biol* **137**, 953–963.

Saruta T (1996). Mechanism of glucocorticoid-induced hypertension. *Hypertens Res* **19**, 1–8.

Selakovic V (2004). Cortisol in plasma and cerebrospinal fluid of patients with brain ischemia [In Serbian]. *Med Pregl* **57**, 354–358.

Shatney CH & Lillehei RC (1982). The influence of megadose methylprednisolone on experimental myocardial infarct size. *Adv Shock Res* **8**, 187–193.

Shen T, Horwitz KB & Lange CA (2001). Transcriptional hyperactivity of human progesterone receptors is coupled to their ligand-dependent down-regulation by mitogen-activated protein kinase-dependent phosphorylation of serine 294. *Mol Cell Biol* **21**, 6122–6131.

Simionescu M & Simionescu N (1991). Endothelial transport of macromolecules: transcytosis and endocytosis. A look from cell biology. *Cell Biol Rev* **25**, 5–78.

Vorbrodt AW & Dobrogowska DH (2003). Molecular anatomy of intercellular junctions in brain endothelial and epithelial barriers: electron microscopist's view. *Brain Res Brain Res Rev* **42**, 221–242.

Zhou J & Cidlowski JA (2005). The human glucocorticoid receptor: one gene, multiple proteins and diverse responses. *Steroids* **70**, 407–417.

Acknowledgements

This research was supported by SFB487 grant from the Deutsche Forschungsgemeinschaft to D.D., SFB688 grant from the Deutsche Forschungsgemeinschaft to C.F. and J.W., and the Reintegration grant MERG-CT-2004-510649 of the European Commission to C.F. The authors are grateful to Eva-Maria Klute for excellent technical assistance.